JOINT EUROPEAN TORUS

JET–P(87)53

R. Gianella

High Resolution X-Ray Spectroscopy at JET

High Resolution X-Ray Spectroscopy at JET

R. Gianella

JET-Joint Undertaking, Culham Science Centre, OX14 3DB, Abingdon, UK

Preprint of an Invited Paper presented at the
9th International Colloquium on UV and X-Ray, Beaulieu-sur-Mer, France
9th - 11th September 1987

1. INTRODUCTION

Diagnostics of the ion distribution functions in the present generation of tokamak devices requires the use of several approaches based on a large variety of experimental techniques and relies on a number of different physical assumptions. In fact, the simultaneous use of different methodologies allows a cross-check of various results and extends the accessible plasma parameter ranges. Also the results of other diagnostics measuring different plasma parameters and an extensive use of numerical simulations are often needed in the process of data validation.

Among these techniques, analysis of the Doppler broadenings and shifts of emission lines are highly valuable [1-2]. The bent crystal spectrometers operating in the soft X-ray region display very good resolution and luminosity performances in this spectral domain typical of the line emission from the central hottest regions of these multi-keV plasmas. Furthermore the simple inverse dependence of the throughput of these instruments on their focal length allows to devise rather unconventional large scale lay-outs such as to meet the needs of complicated and often hostile operational conditions [3].

The main objective of the high resolution ($\lambda/\Delta\lambda = 20000$) X-ray crystal spectrometer installed at JET in 1986, (a 25 metre curvature radius Johann type instrument) is not atomic physics investigations or studies of pollution of that plasma by impurities, but diagnostics of ion populations reliably performed on a routine basis and for different experimental conditions. This is required both in the present operational phase and in the planned deuterium-tritium (D-T) phase.

In this note a short description of the experimental conditions as well as details of the instrument and its lay-out are given in Section 2. In Section 3 some of the observed spectra, and the related simulation studies, are shortly discussed. Finally in Section 4 some of the results from the velocity measurements and the related phenomenology are outlined.

2. EXPERIMENTAL CONDITIONS

JET (Joint European Torus) is the tokamak producing the largest reported laboratory plasmas; its parameters are believed to be the closest realized so far to those of the future fusion reactor [4]. The main objective of this device is to further improve its performance to reach a regime where it should be possible, in a deuterium-tritium plasma, to study the confinement of the thermonuclear alpha-particles produced and their contribution to plasma heating.

JET discharges are characterized by major radii ranging between 2.5 and 3.4 m and circular or D shaped cross sections of area between ~ 2 and ~ 8 m^2. Electron peak densities in the range 1.5 to $6 \cdot 10^{19}$ m^{-3}, electron and ion peak temperatures in the range 1.8 to 7 keV and 1.5 to 15 keV respectively, plasma currents between 1 and 5 MA and toroidal magnetic fields in the range 1.7 to 3.5 T are the main parameters of most of the plasmas studied, under different operating conditions, in the first four years of operation.

Besides the ohmic heating of the plasma, additional heating is supplied by several megawatts of electromagnetic waves in the ion cyclotron range of frequency [5]. Alternatively or in addition to the radio-frequency waves, beams of energetic (~ 80 keV) neutral hydrogen or deuterium atoms are injected into the plasma to increase its energy content [6]. Reference will be made in the following to the influence of these heating systems upon the rotation of the plasma about the torus axis of symmetry.

Several measures are taken at JET to minimize plasma impurities of strongly radiating metal ions. These measures include use of carbon limiters on the plasma outer equatorial plane, coverage with protection carbon tiles of large areas on the Inconel vacuum vessel internal wall to avoid contact with the plasma, carbonization treatments [6] of all the surfaces inside the discharge chamber. As a consequence, the main impurities in the present hydrogen or deuterium plasmas produced are the light ions of carbon and oxygen (normally about 1% of the electrons) [8] while the concentration of nickel (the main constituent of the Inconel alloy) is usually in the range between 10^{-5} and $5 \cdot 10^{-4}$.

JET is an intense source of neutrons from fusion reactions. Yields up to $3 \cdot 10^{15}$ neutrons per s [4], corresponding to peak fluxes of the order of 10^8 neutrons cm^{-2} s^{-1} in the Torus Hall, have been reported. These fluxes, already adverse to the functioning of photon detectors and requiring heavy shieldings of many equipments located in that hall, are expected to increase by some four orders of magnitude in the planned D-T operation phase, resulting in the absolute impossibility to operate most of the diagnostic apparatuses in that environment. Therefore the analysing and detection sections of any spectrograph suitable for operation in that phase have to be positioned in an adequately shielded location outside the Torus Hall.

These requirements determined the design of the curved crystal X-ray spectrometer installed at JET. Its purpose is the ion temperature and plasma rotation diagnostics through the analysis of line profiles and shifts in narrow spectral intervals about the resonance transitions of He-like and H-like ions. The lay out of this instrument is schematically shown in fig. 1. The line of sight, lying in the tokamak equatorial plane, is not directed along a major radius of the toroidal discharge chamber, but its distance from the torus axis is b = 182 cm resulting in a relative Doppler shift $(\Delta\lambda/\lambda)_D$ proportional to the angular velocity ω_Φ of the emitting ions about the mentioned axis according to the relation

$$\left(\frac{\Delta\lambda}{\lambda}\right)_D = \frac{b}{c}\cdot\omega_\Phi = 6.1\cdot10^{-9}\,\omega\ [s^{-1}]$$

where c is the speed of light.

The bent crystal is mounted on a turntable inside a vacuum box positioned just outside a penetration in the three metre thick concrete wall that encloses the Torus Hall; it views the plasma through a beryllium window 0.15 mm thick located at one of the main tokamak ports. The ray path is within an evacuated 30 cm diameter tube connecting the window to the vacuum box. After diffraction from the crystal the X-rays reach the detector via another tube pivoted to an axis next to the crystal box to match the diffracted X-rays direction according to the Bragg angle fixed by the crystal orientation.

Main geometrical constraints imposed by this lay-out are the following:

- source to crystal distance $D = 20$ m;
- Bragg angle range $\theta = 48.75°$ to $52.75°$;
- window extension in the diffraction plane $s = 20$ cm;

they imply the following instrument parameters:

- crystal radius of curvature $R = 25.25$ m;
- fractional linear dispersion $(1/\lambda)\,(d\lambda/dx) \simeq 4\cdot10^{-4}\ cm^{-1}$;
- spectral range observable at one time $(\Delta\lambda/\lambda)_F \simeq 0.8\%$.

The detector, 9 cm high and 25 cm wide, is a multi-wire proportional chamber where each anode wire is connected to a separate amplification and counting chain, thus providing a high count rate (up to 250 kHz per wire) position sensitive photon detection. The anode spacing of 0.127 cm is the dominant resolution limiting factor of the whole instrument. The diffracting area of the crystal is 5 cm high and 12 cm wide. A quartz crystal cut parallel to the planes $22\bar{4}3$ has been used during the first year of operation of the spectrometer. This crystal has been recently substituted with a 440 germanium one in order to increase, due to the higher reflectivity of germanium, the overall luminosity of the instrument from $\sim 5\cdot10^{-13}\ m^2$ str to $\sim 2.5\cdot10^{-12}\ m^2$ str. Accordingly, the time resolution for the ion temperature measurement from the Voigt fit of He-like Ni resonance line, ranging so far between about 20 ms and a few seconds, is expected to improve by a factor of five, if the concentration of that impurity inside the plasma does not vary.

The large focal length of this instrument easily allows accurate direct measurement of the Bragg angle within a few hundredths of a degree provided that care is taken to have precise parallelism between the crystal surface and the atomic planes. This resulted in an estimated relative error on the absolute measured wavelengths of about 0.06% when also the other error contributions (such as those due to the uncertainty on the crystal lattice parameters and the mechanical and encoding inaccuracies) are taken into account.

A more extensive description of this instrument will be published.

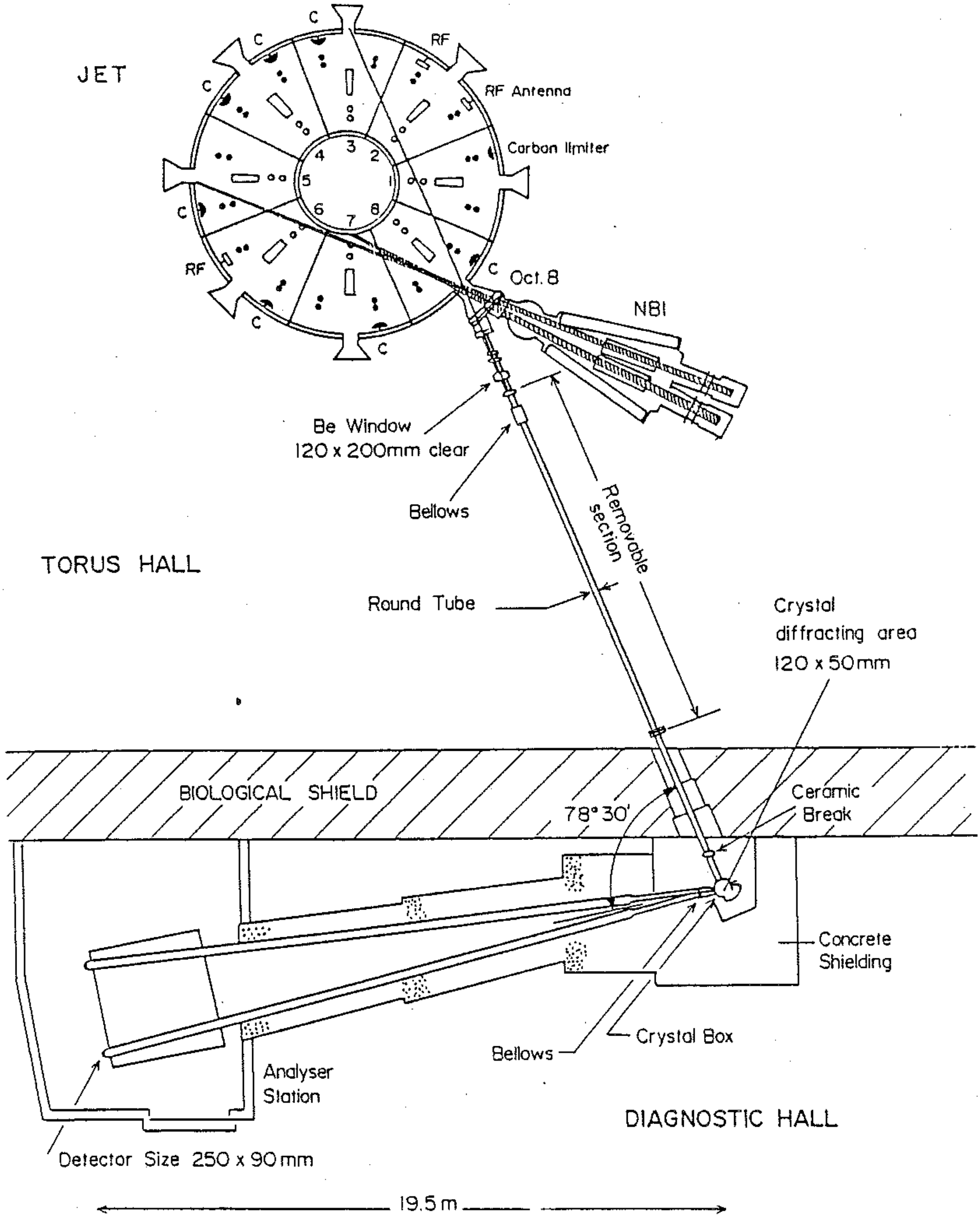

Fig. 1 Schematic lay-out of the X-ray crystal spectrometer installed at JET. The line of sight through the plasma is also shown.

3. SPECTRA

Figure 2 shows an observed spectrum including the resonance line of the He-like nickel. It was recorded by setting the instrument at five different positions in a sequence of repetitive discharges. The central plasma parameters for these discharges were $n_e \simeq 2 \cdot 10^{19}$ m^{-3} and T_e

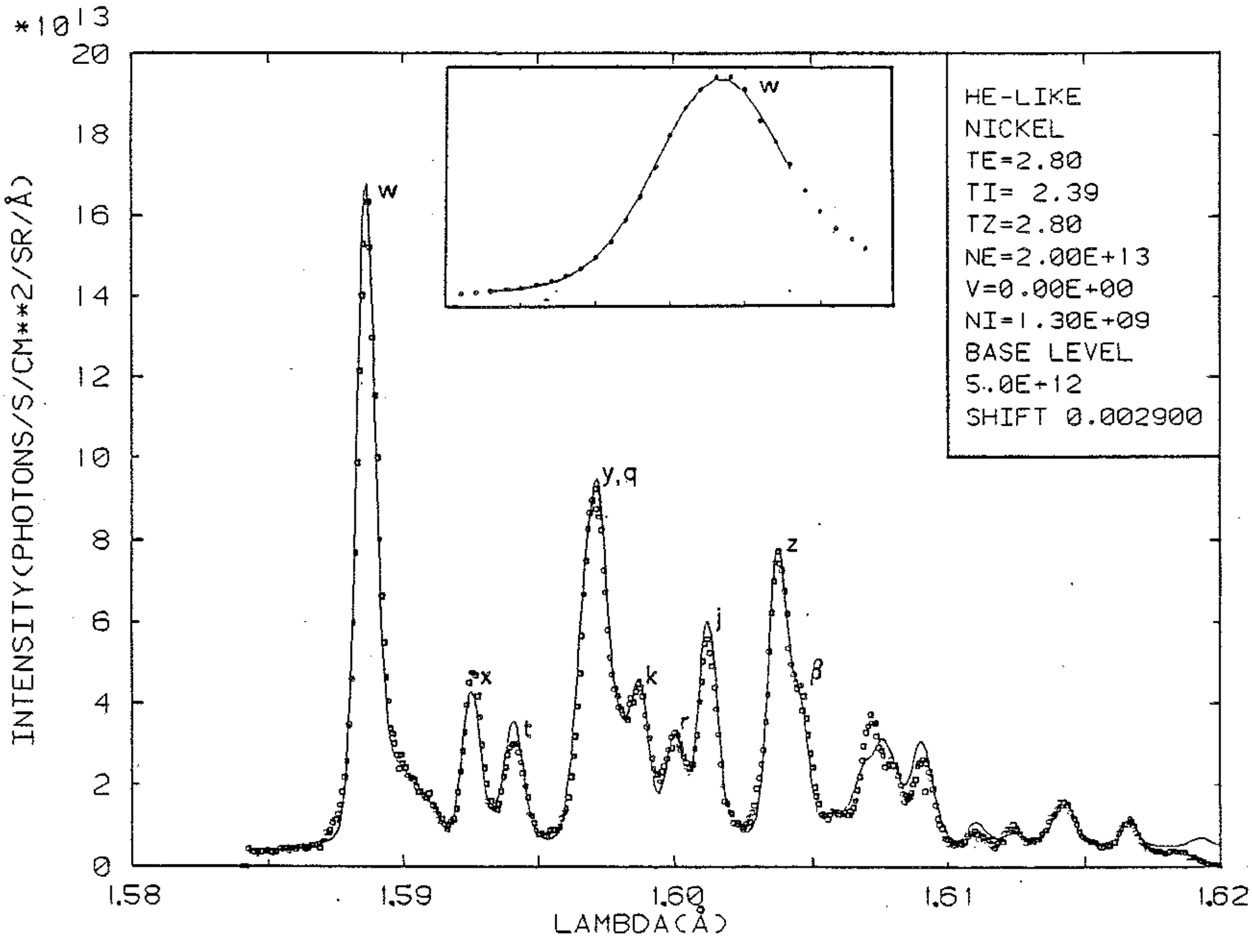

Fig. 2 Experimental resonance spectrum of He-like nickel (boxes) and simulated spectrum (continuous line). The integration time was 9 s. The inset shows the Voigt profile fitting the w line experimental data. (from Ref. [9])

= 3.1 ± 0.3 keV. The wavelength scale, deduced by the instrument setting, is affected as mentioned by an offset error of about 1 mÅ, but the error upon the wavelength separation between peaks is more than ten times smaller. The data in the different segments have been normalized with respect to each other by multiplication by factors ranging between 1.03 and 0.79. All the main spectral features have been identified as lines emitted from nickel ions with two, three, four and five electrons[9]*. The Ni ion temperature as determined from the Voigt fit of the resonance line is 2.4 keV; the fit is shown in the figure inset.

In fig. 3 the Ni H-like resonance spectrum is shown. It was acquired in two consecutive discharges with T_e = 4.7 keV and $n_e = 1.5 \cdot 10^{19}$ m^{-3}. The two Ly-α lines clearly emerge from the continuum background: their intensity ratio is r ≃ 0.6 and the ion temperature from the Voigt fit of Ly-α_1 line is 4.0 keV.

In figs 2 and 3 simulated spectra are overlapped to the observed ones. In the simulation the brightness B_i, as viewed by the spectrograph, for the i-th line making up the spectrum is computed as

$$B_i(\lambda) = \frac{1}{4\pi} \int dx\, \varepsilon(x)\, W_\Delta\left(\frac{\lambda - \lambda_i(x)}{\Delta(x)}\right),$$

* Another study of the He-like Ni resonance spectrum, observed on the TFTR tokamak, including satellites from the three electron system has recently been published [10].

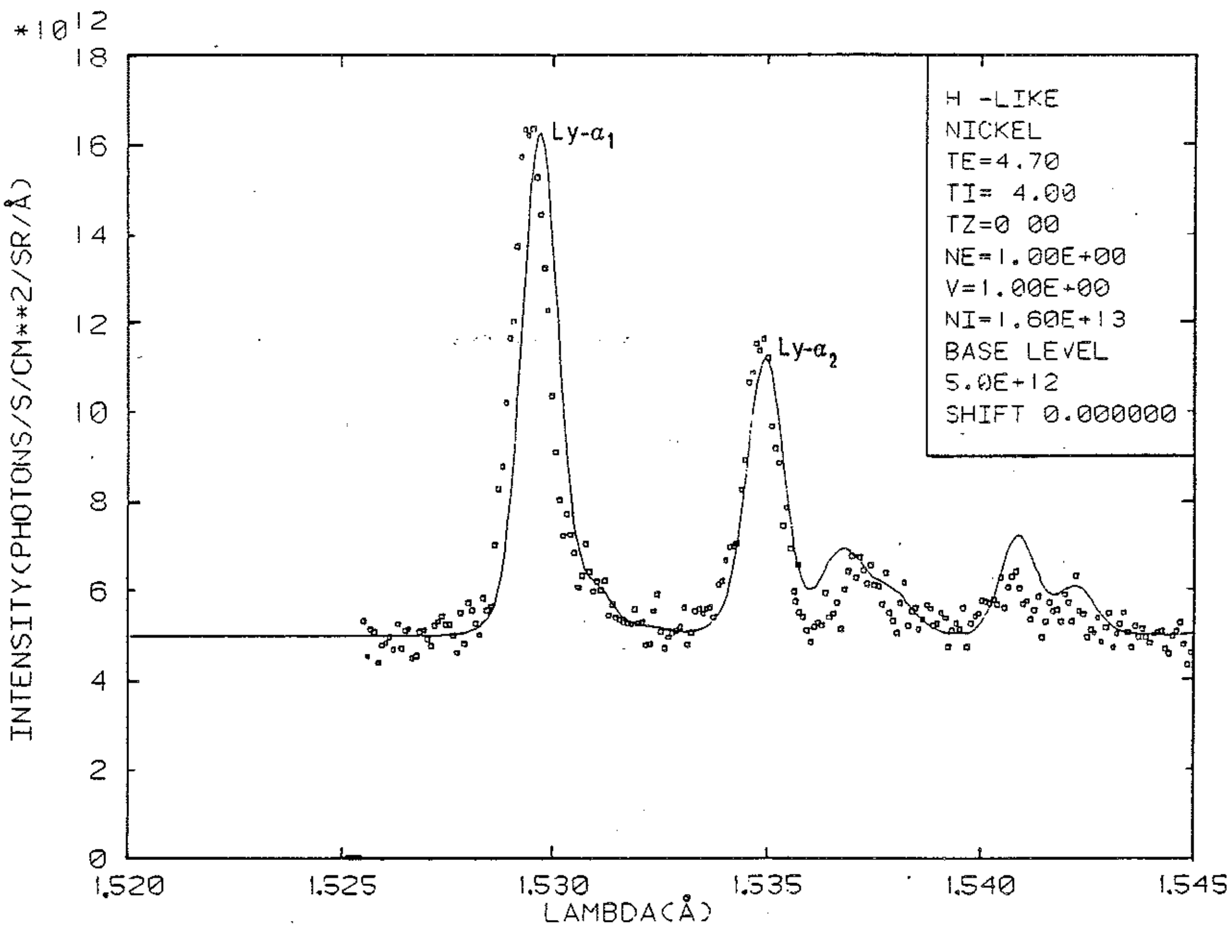

Fig. 3 Experimental resonance spectrum of H-like nickel (boxes) and simulated spectrum (continuous line). The integration time was 10 s. (from Ref [9]).

where the integral is performed along the line of sight and ε is the emissivity depending upon the local plasma parameters. In doing this, use is made of the results supplied by other diagnostics independently measuring the electron temperature [11] and density [12] at the different plasma positions. These quantities allow a calculation of relative abundancies of the different ionization stages at the various positions according to the coronal ionization-recombination mechanisms and suitable modelling of the transport of these ions across the discharge. The width Δ appearing in the equation for the spectral brightness and the central apparent wavelength λ_i in the spectral shape function W_Δ are also dependent upon the position through the local ion temperature and bulk velocity respectively. The bulk velocity of the ions is assumed directed toroidally and can be set to vary with the torus major radius. For purely ohmically heated discharges like those referred to by figs 2 and 3 the rotation velocity is very small compared to the error on the absolute wavelengths measure and is therefore set to zero in the simulations displayed.

A detailed comparison of the experimental spectra with theoretical atomic data has been performed and published [9]. Here we limit ourselves to a few remarks. In the simulation of fig. 2* (taken from Ref. [9])a central electron temperature of 2.8 keV** was assumed to get a

* 148 lines are included in this simulation. The atomic data describing the principal mechanisms of population of levels in the transitions considered have been expressely computed by F. Bely-Dubau, M. Cornille, J. Dubau, P. Faucher and A.H. Gabriel using the computer packages SUPERSTRUCTURE [13] of the University College of London and AUTOLSJ [14] of the Meudon Observatory.

** This value is consistent with the quoted electron temperature measurement within its estimated error.

better reproduction of the intensity ratios between the k and j dielectronic satellites and the resonance line w.* The concentrations of the Li-, Be- and B-like ions needed to be increased by factors of about 2 with respect to the values deduced by coronal equilibriumcalculations [16] in order to reproduce more accurately the spectral features depending upon the density of these ions.

Several possible reasons have been considered to explain the discrepancy between the coronal prediction and the experimentally observed concentrations of the lower ionization stages. They include possible errors in the temperature measurements, uncertainties in the ionization, recombination, excitation rates and radiative probabilities, effects due to possible hollow concentration profiles of the Ni impurity in the plasma column, effects due to charge exchange with neutral hydrogen and deuterium atoms present mainly in the cooler outer regions of the plasma column, where the lower ionization stages are more abundant, and possibly transport of the impurities across the plasma.

The simulation of fig. 3 results from the integration along the instrument line of sight of the emissivities of 74 transitions of the one and two electron systems of Ni; in particular the magnetic dipole transition (2s $^2S_{1/2}$ - 1s $^2S_{1/2}$) is blended with the Ly-α_2 line contributing about

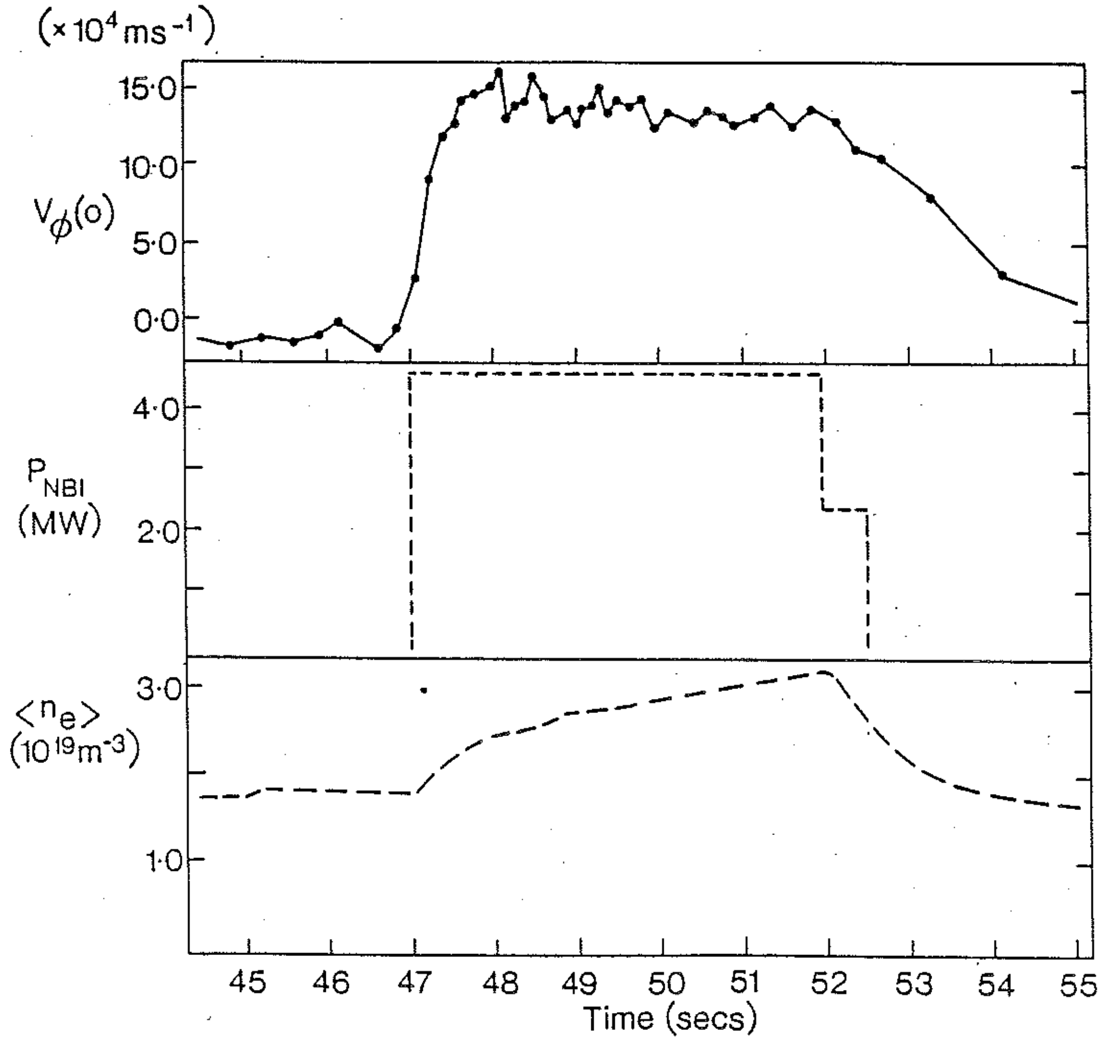

Fig. 4 Response of the central plasma rotation velocity $v_\phi(0)$ to *co-injection* of neutral beams of power P_{NBI}. Positive values of v_ϕ indicate toroidal rotation in the *co-direction*. The average electron density behaviour is also displayed.

* The alphabetic notation introduced by Gabriel [15] is used here and in fig. 2.

ten percent to the intensity of the latter, whose value is calculated to be 0.5 times that of the Ly-α_1 in the actual plasma conditions [17-18].

4. VELOCITY MEASUREMENTS

Among the diagnostic applications of this instrument, besides the capital information about the ion temperature at the plasma centre or that about electron temperature, impurity concentrations and ionization balances, it is important the information deduced from the measurement of the plasma toroidal angular velocity. During the purely ohmic heating phases of the discharges the plasma is seen to rotate in the direction opposite to that of the toroidal plasma current (the counter-direction) by an amount (ω_ϕ = 4 to $8 \cdot 10^3$ s^{-1}) just above our instrumental detectability. But when the neutral beams are fired they apply a net torque to

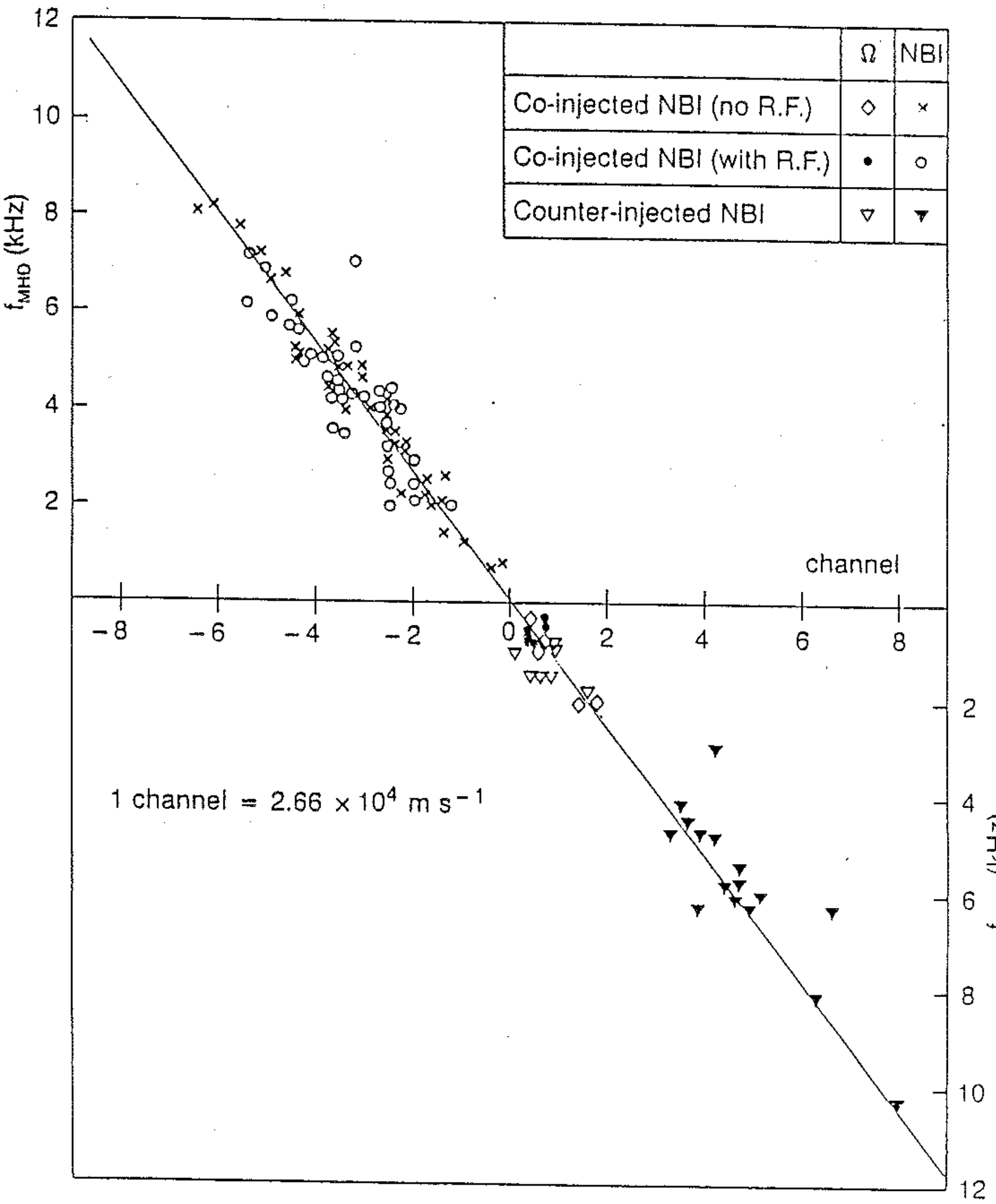

Fig. 5 The frequency of MHD n = 1 oscillations vs the Doppler shift of the He-like Ni resonance line measured in channels at the detector. The line across the experimental data represents the equation $2\pi f_{MHD} = \omega_\phi$. (from ref. [20])

the plasma so that the latter is observed to speed up on a time scale of about 1 s reaching angular velocities up to $\omega_\phi = 8 \cdot 10^4\ s^{-1}$in the co- or counter-direction according to the beams orientation relative to the plasma current (see for example fig. 4).

It may be interesting to mention the strong correlation found at JET between the fluid velocity as measured by this instrument and the n = 1 magnetohydrodynamic (MHD) oscillations. These phenomena are due to deformations of the axisymmetric structure of the plasma caused by MHD instabilities [19]. The n number is the integer ratio between the torus large circumference and the spatial period of these perturbations along that circumference. The frequency of the oscillations, as measured by means of fixed probes, can be interpreted as due to a rotation of the perturbation pattern. When such perturbations were detected with amplitude at the plasma edge larger than 10^{-4} times the stationary field, the apparent rotation speed of the n = 1 modes both internally (as detected by the electron cyclotron emission measurements [9]) and externally located (measured with magnetic probes) was seen to be very close to the central fluid speed (see fig. 5). This coincidence was observed both in ohmic phases at low rotation speed and at large speed when the neutral beams were injected into the plasma [20].

Further evidence of the close coupling of the MHD modes with the fluid translation motion is given at the occurrence of the so-called mode lockings [21]. Under certain circumstances, in fact, the mentioned modes are slowed down until the n = 1 magnetic perturbation *locks* to the external structure. These events also happen during the neutral beams injection. In these cases also, the plasma toroidal velocity has been observed to slow down from values comparable to the fluid sound speed to zero on a time scale of 0.1 s, not withstanding the persisting action of the beams [20].

CONCLUSIONS

High resolution X-ray spectroscopy has been applied to diagnose the plasmas produced by JET. The spectroscopic equipment functioned routinely during 1986 to monitor the central ion temperature and the plasma toroidal rotation. Its particular lay-out should allow operation into the future D-T phase.

Emission spectra including lines from nickel ions H-like to B-like were resolved for the first time and compared with theoretical computations. Absolute wavelength measurements with relative uncertainties lower than 1/1500 have been performed.

Investigation of the relationship between data from this diagnostic methodology and other measurements allowed descriptions of remarkable phenomena as well as to judge the merits of the different operating scenarios.

ACKNOWLEDGEMENTS

The high resolution spectrometer was proposed, designed and built by CRE Frascati of ENEA supported by JET under several contracts. The exploitation and interpretation of data from the X-ray crystal spectrometer is due to the collaboration of teams from the Frascati and JET laboratories to whom the author of this note is indebted. In particular thanks are due to R. Bartiromo, K. Behringer, F. Bombarda, F. De Marco, W. Engelhardt, N. Foden, E. Källne, G. Magyar, S. Mantovani, B. Oliver, L. Panaccione, G. Pizzicaroli, D. Schram, M. Shaw, J. Snipes, D. Stork, H. Summers, G.J. Tallents, G. Tonetti and B. Viaccoz.

REFERENCES

[1] M. Bitter et al., Phys. Rev. Lett., **42** (1979) 304

[2] M. Bitter et al., in *Temperature, its Measurements and Control in Science and Industry*, ed. by J.F. Schooley (AIP, New York, 1982) **5**, 693

[3] R. Bartiromo et al., Nucl. Instrum. and Methods, **225** (1984) 378

[4] P.H. Rebut and P.P. Lallia, Proc. 7th Int. Conf. on Plasma Phys. (Kiev, URSS, 6-10 April 1987)

[5] J. Jacquinot et al., Proc. 11th Int. Conf. on Plasma Phys. and Controlled Nucl. Fusion Research (Kyoto, Japan, 13-20 November 1986) IAEA-CN-47/F-I-1

[6] G. Duesing et al., Phil. Trans. R. Soc.London **A322** (1987) 109

[7] J.P. Coad, K.H. Behringer and K.J. Dietz, J. Nucl. Mat. **145-147** (1987) 747

[8] K. Behringer et al., Proc. 11th Int. Conf. on Plasma Phys. and Controlled Nucl. Fusion Research (Kyoto, Japan, 13-20 November 1986) IAEA-CN-47/A-IV-1

[9] F. Bombarda et al., Phys. Rev. A, in press 1987

[10] H. Hsuan et al., Phys. Rev. A, **35** (1987) 4280

[11] D.V. Bartlett, E.A.M. Baker, D.J. Campbell, A.E. Costley, Rev. Sci. Instrum., **56** (1985) 940

[12] D. Veron, Int. School of Plasma Phys., Workshop on Diagnostics for Fusion Reactor Conditions (Varenna, Italy, 6-17 September 1982) Eur 8351-II-EN p. 283

[13] W. Eissner, M. Jones, H. Nussbaumer, Comput. Phys. Commun. **8** (1974) 270

[14] TFR Group, J. Dubau and M. Loulergue, J. Phys. B, **15** (1981) 1007

[15] A.H. Gabriel, Mon. Not. R. Astr. Soc., **160** (1972) 99

[16] IonizationRates from A. Burgess and M.C. Chidichimo, Mon. Not. R. Astr. Soc., **203** (1983) 1269

Radiative Recombination Rates from S. Von Goeler et al., Nucl. Fusion, **15** (1975) 301

Dielectronic Recombination Rates from D.E. Post et al., At. Data Nucl. Tables, **20** (1977) 397

[17] G.J. Tallents, J. Phys. B, **18** (1985) 3299

[18] N.N. Ljepojevic, R.W.P. Mc Whirter, S. Volontè, J. Phys. B, **18** (1985) 3285

[19] H.P. Furth, Phys. Fluids, **28** (1985) 1595

[20] D. Stork et al., 14th Europ. Conf. on Contr Fus. and Plasma Phys. (Madrid, Spain, 22-26 June 1987) Vol. 11D, I, 306

[21] J.A. Snipes et al., 14th Europ. Conf. on Contr Fus. and Plasma Phys. (Madrid, Spain, 22-26 June 1987) Vol. 11D, I, 69